Carbohydrate Polymers 132 (2015) 25–30

Contents lists available at ScienceDirect

Carbohydrate Polymers

journal homepage: www.elsevier.com/locate/carbpol

NaOH treatment of chitosan films: Impact on macromolecular structure and film properties

E.A. Takara, J. Marchese, N.A. Ochoa *

Instituto de Física Aplicada (INFAP), Departamento de Química—Universidad Nacional de San Luis, CONICET, Chacabuco 917, CP: 5700 San Luis, Argentina

ARTICLE INFO

Article history:
Received 13 March 2015
Received in revised form 27 May 2015
Accepted 30 May 2015
Available online 10 June 2015

Keywords:
Chitosan
Polymorphs
Deacetylation
Deprotonation

ABSTRACT

In this paper, we examine the significance of treatment with NaOH on chitosan (CH) film structure to obtain biodegradable materials for several applications. In order to determine the structure of the films, an analysis based on SEM, FTIR spectroscopy and X-ray diffraction data was performed. In addition, the consequences of this treatment were evaluated by swelling index measurements and mechanical testing. As result of FTIR and X-ray analysis, three effects were identified: the deprotonation and phosphate extraction, which allowed new hydrogen bonds to form, and a higher CH deacetylation. These studies also revealed that two hydrated and anhydrous polymorphs were present in the CH–NaOH films. Moreover, the new hydrogen bond and the reduction of *N*-acetyl groups produced films with a more compact and disordered structure, reducing their swelling characteristics and increasing their brittleness. The introduction of a mild NaOH treatment is a versatile tool to obtain chitosan films with interesting and tunable properties.

1. Introduction

Chitosan (CH) is a linear copolysaccharide β-(1 → 4)-2-amine-2-deoxy-*d*-glucose (GlcNac) and β-(1 → 4)-2-acetamine-2-deoxy-*d*-glucose (GlcN). It is biodegradable, non-toxic, bio-compatible, and renewable (Croisier & Jérôme, 2013; Sevel, Ikinci, & Kas, 2000; Kaminski & Modrzejewska, 1997). Also, it can be easily modified and has a noticeable ability to form many complexes with metal ions and enzymes (Schmuhl, Krieg, & Keizer 2001; Khor, 1997). In addition to its many uses in food and agricultural applications, CH exhibits the ability to form films. CH is obtained from chitin, which is mainly extracted from crustacean exoskeletons (Kurita, 2006; Muzzarelli, 1973). The solubility of polymers in aqueous acidic media solutions has been used to distinguish chitin from CH. The word chitosan has been used for soluble polymers obtained from the deacetylation of chitin. Incomplete deacetylation reaction allow for the aleatory distribution of GlcNac and GlcN residues (Abdou, Nagy, & Elsabee, 2008; Chang, Tsai, Lee, & Fu, 1997; Knaul, Kasaai, Bui, & Creber, 1998; Tolaimatea et al., 2000). The degree of deacetylation (DD) determines some of the characteristics of CH, such as solubility, biodegradability, and aggregation properties (Cho, Jang, Park, & Ko, 2000; Kubota & Eguchi, 1997; Kristiansen, Vårum, & Grasdalen, 1998; Liu et al., 2003; Schatz, Pichot, Delair, Viton, & Domard, A. 2003). DD below 40–50% yields soluble polymers (Wang et al., 2008, 2006). Extensively solubility studies have been carried out and confirmed that the solubility decreases as DD decreases. The results obtained by Franca, Freitas, and Lins (2011) using molecular dynamics simulations support the hypothesis that the solubility of CH is controlled mainly by electrostatics interactions and water molecules mediate polymer aggregation. The water molecules interact with the acetyl and/or protonated amino groups. Hydrolysis of CH affects the crystalline structure of this biopolymer, and the resulting crystallites can be used as fillers in attractive composite materials (Gopalan & Dufresne, 2003; Paillet & Dufresne, 2001; Morin & Dufresne, 2002; Phongying, Aiba, & Chirachanchai, 2007; Struszczyk, 2006). In 1936, Clark and Smith (Yui et al., 1994) reported the first X-ray diffraction pattern of CH. In 1997, Okuyama (Okuyama, Noguchi, Miyazawa, Yui, & Ogawa, 1997) described the CH structure as a two-fold helix in a zigzag. These chains extend along to axis *c* (fibre axis) and are arranged in an antiparallel fashion. The unit cell dimensions were $a = 8.95$, $b = 16.97$, and $c = 10.34$ Å, and it was stabilised by O3•••O5 hydrogen bonds. There are also eight water molecules in the unit cell, which is why it is called a hydrated tendon polymorph. When hydrated CH is annealed at 200 °C other polymorph appears, which results from the loss bound water, and is called an anhydrous polymorph (Yui, Ogasawara, & Ogawa, 1995; Okuyama, Noguchi, Hanafusa, Osawa, & Ogawa 1999; Okuyama et al., 1997). Like the hydrated form, the anhydrous

* Corresponding author. Tel.: +54 2664446211; fax: +54 2664435630.
E-mail address: aochoa@unsl.edu.ar (N.A. Ochoa).

http://dx.doi.org/10.1016/j.carbpol.2015.05.077
0144-8617/

polymorph has a two-fold helix in a zigzag structure arranged in an antiparallel fashion. However, due to the loss of bound water, new interchain hydrogen bonds are formed. The removal of bound water and the formation of hydrogen bonds is an irreversible process (Ogawa, Yuib, & Okuyamac, 2004) that involves strong O3•••O5 and weak O3•••O6 hydrogen bonds within the unit cell. It has been reported that anhydrous polymorphs present low biological and chemical reactivity (Harish Prashanth, Kittur, & Tharanathan, 2002). Ogawa, Yui, and Miya (1992) and Saito, Tabeta, and Ogawa (1987) confirmed that the crystalline structure of CH depends on the preparation method used. Extensive research has been carried out on acid hydrolysis of CH in solution and in a solid state (Osorio-Madrazo et al., 2010). However, there are a few reports on the CH polymorph structure after treatment with NaOH in a solid state. In this paper, we examine the significance of NaOH treatment on the CH film structure. In order to reveal the structure of films, an approach based on FTIR spectroscopy and X-ray diffraction analysis was performed. Water uptake, solvent solubility, and mechanical properties of CH and CH–NaOH films were also determined.

2. Experimental

2.1. Materials

A commercial sample of CH powder of average viscometer molecular weight (890 kDa), with approximately 75% deacetylation, was supplied by Sigma-Aldrich. The following analytical grade chemicals were also purchased from Sigma-Aldrich: NaOH (98%), *ortho*-phosphoric acid (85%), glycerol, acetone, ethanol, *N*,*N*-dimethylformamide, and chloroform. All solutions were prepared with Milli-*Q* water (resistivity > 1.8 mΩ).

2.2. Preparation of CH film

CH film was prepared by dissolution in 50 mL of 1% aqueous phosphoric acid solution. CH was added to prepare 2% of biopolymer solution and then glycerol was used as plasticiser (0.5%). The films were cast in Petri dishes (14.5 cm internal diameter) and dried in an oven at 40 °C for 48 h. To neutralise the matrix polymer and remove the excess acid, the membrane was immersed in solutions of NaOH. The concentration the NaOH and contact time was varied between 0 and 1 M of NaOH and 24–72 h, respectively. Finally, the films were washed with deionised water to neutrality. Film preparation was carried out in triplicate.

2.3. Membrane characterisation

2.3.1. Scanning electronic microscopy (SEM)

Electron micrographs were obtained by a scanning electron microscope LEO 1450VP. The membranes were fractured in liquid nitrogen and mounted on sample holder previous coverage with a conductive material. SEM imaging was examined using an accelerating voltage of 10 kV.

2.3.2. X-ray diffractometry (XRD)

The crystalline structures of the membranes were characterised with a Rigaku model D-Max III C X-ray diffractometer with a θ angular range from 5° to 60°, operated at 30 kV (λ = 0.15418 nm), with a Cu*K*-λ light and nickel filter. The relative intensity was taken at room temperature with a step size of 0.02. The samples were cut into rectangles of 7 × 12 mm and dried at 60 °C for 48 h. From the diffractograms, the *d*-spacing (d_{sp}) of each synthesised film was determined using Bragg's equation (Eq. (1)), taking the highest-intense peak as reference ($2\theta \cong 20^\circ$).

$$n\lambda = 2d\ \sin\theta \tag{1}$$

The crystallinity index (CrI) was determined according to the method proposed for cellulose (Segal, Creely, Martin, & Conrad, 1959) and applied to CH (Struszczyk, 1987) by using the following equation:

$$\mathrm{ICr}\,(\%) = \frac{I_{110} - I_{\mathrm{am}}}{I_{110}} \times 100 \tag{2}$$

where I_{110} is the maximum intensity of the reflection at $2\theta \cong 20^\circ$ and I_{am} is the minimum intensity of diffraction in the amorphous region.

Peak broadening of the XRD reflection was used to calculate the mean crystallite size (D) using the Scherrer formula (Azaroff, 1968), which is given in the following equation:

$$\Delta\left(2\theta\right) = \frac{0.9\lambda}{D\cos\theta} \tag{3}$$

where λ is the X-ray wavelength of the Cu *K*α radiation (=1.54 Å), β is the full-width at half-maximum of XRD peaks and θ is the diffraction angle.

2.3.3. Infrared spectroscopy

FTIR spectra were determined using an FTIR Varian 640 Spectrometer using ATR mode. The obtained spectrum had a resolution of 4 cm^{-1} and consisted of approximately 3500 points, and had integration times of 60 s (1 s per scan). The number of scans for each sample was 64. The samples were dried at 60 °C for 48 h and made into a homogeneous powder by milling.

To determine the degree of deacetylation in the films (CH–NaOH), the original spectrum was analysed. The degree of deacetylation (DD) was obtained from the Brugnerotto equation (Brugnerotto et al., 2001):

$$\mathrm{DD}\,(\%) = 1 - \left\{31.92\left(\frac{A_1}{A_2}\right) - 12.20\right\} \tag{4}$$

where A_1 is the area of the band located at 1316 cm^{-1} (characteristic band of amide III) and A_2 the area of the reference band at 1423 cm^{-1} (stretching CH band). Similar results were found by using both methods.

2.3.4. Solubility assays (S) and swelling index (SI)

Solubility assays were carried out by treating the films with distilled water for 120 h at temperatures of 25 °C and 50 °C. The swelling index (SI) of the membranes provided an indirect measure of the degree of insolubility of the polymer matrix. An area of 1 cm^2 of each CH–NaOH film was vacuum dried in an oven at 40 °C for 24 h. The dried film was accurately weighed (W_d) and immersed in a flask containing 50 mL distilled water at 25 °C. After 12 h, the swollen samples were removed from the aqueous medium, surface dried to remove excess surface water by light blotting with tissue paper, and weighed (W_w). All experimental trials were carried out in triplicate. The swelling index was determined by the following equation:

$$\%\mathrm{SI} = 100\left(\frac{W_W - W_d}{W_d}\right) \tag{5}$$

2.3.5. Mechanical properties

Tensile tests of the synthesised CH–NaOH films were performed at room temperature using a Comten Industries (Series 94 VC) device (Pinellas Park, Tampa FL, USA) according to ASTM D882 (ASTM, 2010a, 2010b) with some modifications. The films were cut into strips 1.1 cm wide and 4.0 cm long using a sharp scalpel. The ends of the strips were mounted between cardboard grips using double-side adhesive tape. To ensure complete relaxation of the polymeric structures and to standardise the experimental procedure, film samples were stored in a humidity- and temperature-controlled chamber for 24 h at 25 °C and 100% R.H.

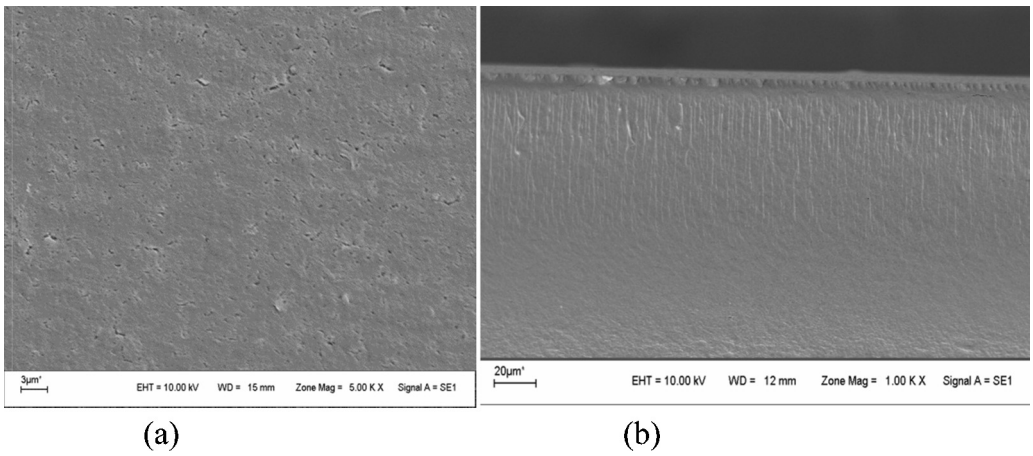

Fig. 1. Top (a) and cross-section (b) of CH–0.5 NaOH film.

Under these conditions (RH = 100%), the CH membrane was too fragile to measure its tensile strength. The polymeric strips were then fixed between upper and lower clamps of the tensile tester and the tensile strength was determined at a constant traction speed of 5 mm/min. The mechanical parameter data include the average values and standard deviation from three samples of each film. The film thickness was measured using a Köfer micrometer (precision ± 1 μm, Germany).

2.3.6. Statistical analysis

Swelling Index and Mechanical properties results were subject to one-way analysis of variance (one-way ANOVA). Comparison of means was carried out by Duncan's new multiple range tests at a confidence level of 95%. All statistical calculations were performed using SPSS for Windows® (SPSS Inc., Chicago, IL). The experimental results are presented as mean values with standard deviations.

3. Results and discussion

3.1. SEM analysis

The scanning electron micrographs of all chitosan films exhibit the same structure, as it is showed in Fig. 1 corresponding to CH–0.5NaOH. It can be seen that the surface present some surface defects. However, cross-section image reveals a dense or compact structure underneath the top layer. That is because the processing technique plays an important role to determine the morphology of films. In general, the asymmetric structure can be resulted of the rapid water evaporation in the interface in the first minutes and then, once the solid top layer is consolidated the sublayers experiment a lower evaporate rate. This changes based on kinetic considerations can qualitatively explain the structure found in these films. Similar structure has been reported by Ma, Li, Qin and He (2013).

3.2. FTIR and X-ray analysis

Fig. 2 shows the FTIR spectra of CH, CH–0.25NaOH, CH–0.5NaOH, and CH–1NaOH. Also, characteristic absorption bands of neat and NaOH treated CH films were resumed in Table 1. In the CH film spectra, a NH_3^+ stretch band appears at 3450–3350 cm^{-1} and overlapped with the —OH stretch band. According to other researchers (Pearson, Marchessault, & Liang, 1960; Pawlak & Mucha, 2003) protonation of chitosan amine functionalities is suggested by the presence of two peaks, both attributed to NH^{+3} groups, namely the antisymmetrical deformation at 1620 cm^{-1} and the symmetric

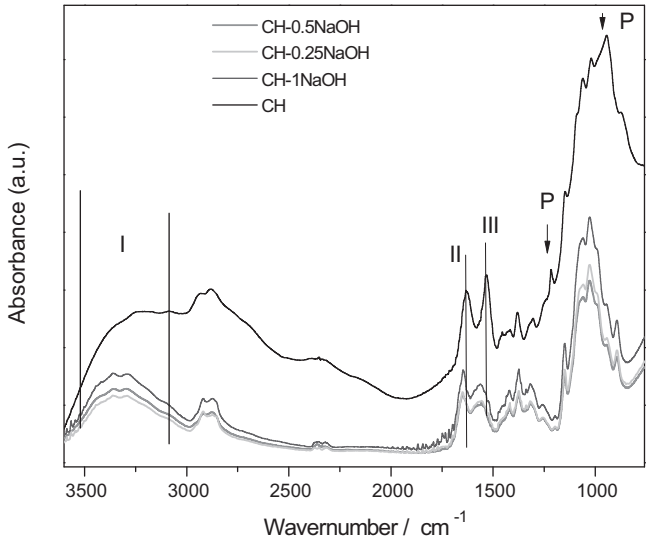

Fig. 2. FTIR spectrums of CH and CH–NaOH films.

Table 1
ATR–FT-IR spectra peak assignments of CH and CH–NaOH.

CH Wave number (cm^{-1})	CH–NaOH Waver number (cm^{-1})	Description
3400	3357	OH hydroxyl group.
3260	3291	NH group-stretching vibration
2922	2919	Symmetric or
2874	2869	asymmetric CH_2 stretching vibration attributed to pyranose ring
1620	1657	C═O in amide group (amide I band)
1530	1562	NH-bending vibration in amide group
1316	1321	NH_2 in amino group
1422	1420	Vibrations of OH, CH in the ring
1381	1375	CH_3 in amide group
1216	–	PO_4^{-3}
1150–1040	1142–1055	—C—O—C— in glycosidic linkage
970–940	970–940	P—O stretching of P—OH, overlap with —CH_3 rocking
870	887	CH_3COH group

Table 2
Degree of deacetylation (DD).

FILM	DD % (degree of deacetylation)
CH	73.73
0.25	75.02
0.5	78.98
1	83.02

deformation at 1530 cm^{-1}. A band at 1216 cm^{-1} was observed, which is attributed to the P═O stretching and the distinctive ν_1 [PO_4^{-3}] vibrational band a 967 cm^{-1}. Electrostatic attraction between the NH^{+3} of CH and the [PO_4^{-3}] may be the main interaction leading to water solubility of CH. The presences of the [$PO4^{-3}$] groups break the intra-molecular hydrogen bonding of CH (Wang & Liu, 2014). Methylene groups presented characteristics bands at 2900 cm^{-1} and at 1466–1377 cm^{-1}. The band at 1320 cm^{-1} corresponded to a C—N bond, and bands at 1078, 1032, and 1105 cm^{-1} were due to asymmetric stretching of both C—O—C and pyranose groups (Liu, Adhikari, Guo, & Adhikari, 2013). In CH–NaOH films, bands I, II, and III shifting were due to amine group deprotonation when films were contacted with NaOH. This deprotonation reduced the hydration shell of the amine groups (Cesteros Iturbe, 2004; Min et al., 2004) and allowed new hydrogen bonds to form in the CH chains. Moreover, phosphate band at 1216 cm^{-1} disappears while the band intensity at 967 cm^{-1} diminishes. These results indicate that NaOH produce deprotonation and phosphate extraction of CH matrix. FTIR study allowed to calculate the degree of deacetylation (DD) of the CH–NaOH films. Table 2 shows that degree of deacetylation increased as the NaOH concentration was increased. CH films treated with aqueous NaOH solutions revealed three effects by FTIR spectroscopy: desprotonation and phosphate extraction, which allowed the formation of new hydrogen bonds and increased CH deacetylation. Ruel-Gariépy, Chenite, Chaput, Guirguis, and Leroux (2000) reported that deacetylation degree reduction can increase the hydrophobic interactions when CH annealing is performed. A similar behaviour can be expected for NaOH-treated films.

XRD studies revealed that changes in the crystalline structure occur when the films were treated with aqueous NaOH solutions. Fig. 3 reveals that the CH film showed the characteristic form of hydrated "tendon" CH. Hasegawa, Isogai, and Onabe (1993) carried out the homogeneous hydrolysis of CH in 85% phosphoric acid at ambient temperatures over 4 weeks. They found that the water insoluble fraction presented an anhydrous pattern, whereas the

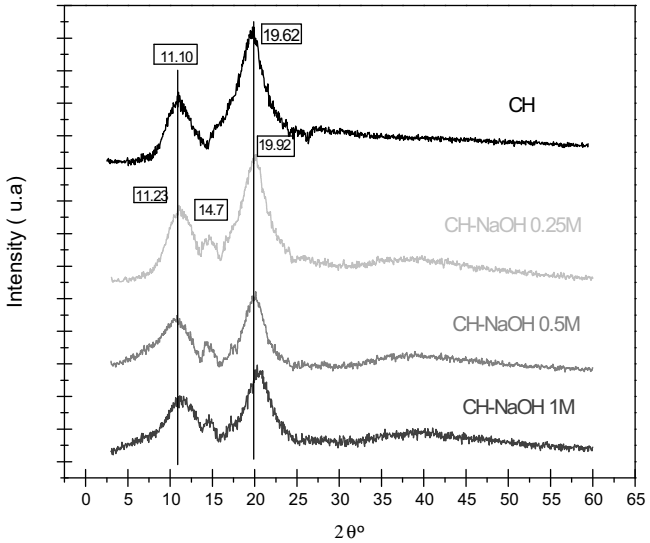

Fig. 3. XRD of CH and CH–NaOH films.

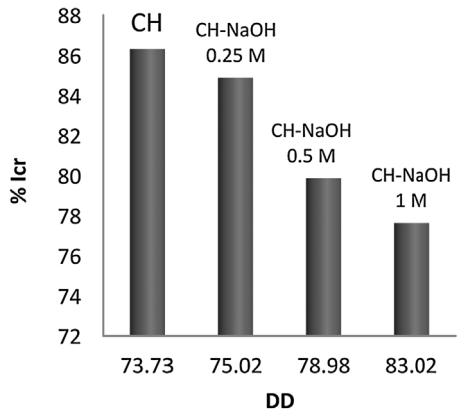

Fig. 4. Influence of DD on CrI.

water soluble fraction showed a hydrated pattern. In this study, the CH film diffractogram presented bands typical of a hydrated polymorph at $2\theta^\circ = 11.1^\circ$ and $2\theta^\circ = 19.62^\circ$ (Saito et al., 1987; Liu et al., 2013; Zhang, Ding, Ping, & Yu, 2006) revealing that the dissolution of CH with diluted phosphoric acid resulted in a hydrated polymorph. In addition, all CH–NaOH films showed other reflection peaks corresponding to anhydrous polymorph at $2\theta^\circ = 14.7^\circ$ (Ogawa et al., 1992; Saito et al., 1987). X-ray diffraction patterns in CH–NaOH films revealed that two crystalline zones were present: hydrated and anhydrous polymorphs. These polymorph combinations are referred as 1–2 (Saito et al., 1987). In Table 3, the *d*-spacing of the films are listed. After NaOH treatment, an increase in NaOH concentration produced films with lower *d*-spacing values, thus indicating that the films were more compacted, due to both hydrogen bonding formation and deacetylation. In order to determinate the crystallinity index (CrI), the procedure described by Osorio-Madrazo et al. (2010) was used. A diminution of CrI was found as NaOH concentration increased.

In Fig. 4, the relationship between CrI and DD can be observed. A diminution of *N*-acetyl groups results in films with more compacted and disordered structure (less hydrated shells were present). Similar results were found by Osorio-Madrazo et al. (2010) for the acid hydrolysis of CH. The apparent width (L_{hkl}) of anhydrous and hydrated crystals was determined by using the Scherrer equation (Table 3) from the reflection of $2\theta^\circ = 14.7$ and $2\theta^\circ = 11$, respectively. The new anhydrous crystal width was higher than the hydrated one when these reflections were compared. Moreover, the anhydrous crystal width increased as the NaOH concentration increased, revealing a growth of this parameter unlike to those of the hydrated phase ones. New hydrogen bonds and fewer acetyl groups caused a larger anhydrous crystal size.

3.3. Solubility, swelling index, and mechanical properties

The importance of *N*-acetyl groups on CH solubility or their capacity to support swelling process has been extensively reviewed (Abd-Elmohdy, Sayed, Essam, & Hebeish, 2010; Panos, Acosta, & Heras, 2008; Nimesh, Saxena, Kumar, & Chandra, 2012; Shi, Neoh, Kang, & Wang, 2006; Cunha et al., 2012). The CH film obtained was water soluble, where as CH–NaOH films were insoluble. Fig. 5 shows the swelling index, indicating that higher concentrations of aqueous NaOH solutions reduced the swelling in the CH–NaOH films. However, the difference between CH–0.5 NaOH and CH–1NaOH was not statistically significant. Franca et al. (2011) indicated that the electrostatic contributions were the main driving force for the aggregation process, while the hydrophobic contributions do not seem to play an important role. This was based on the analysis of free energy solvation of CH. Moreover, these researchers

Table 3
Crystallinity parameters and *d-spacing* of prepared films.

Concentration of NaOH (M)	CrI %	D [nm] $2\theta^{\circ} = 15^{\circ}$	D [nm] $2\theta^{\circ} = 19^{\circ}$	d-Spacing (A°) $2\theta^{\circ} = 15^{\circ}$	d-Spacing (A°) $2\theta^{\circ} = 19^{\circ}$
0	86.31	–	4.95	–	4.524
0.25	84.88	12.77	4.64	5.89	4.456
0.5	79.86	13.91	3.97	5.88	4.441
1	77.63	16.69	3.69	5.82	4.347

$d_{15^{\circ}}$ [A°] = d-spacing of the anhydrous polymorph; $d_{19^{\circ}}$ [A°] = d-spacing of the hydrated polymorph. $D_{15^{\circ}}$ [nm] = crystallite size anhydrous polymorph; $D_{19^{\circ}}$ [nm] = crystallite size hydrated polymorph; CrI = percentage crystallinity index.

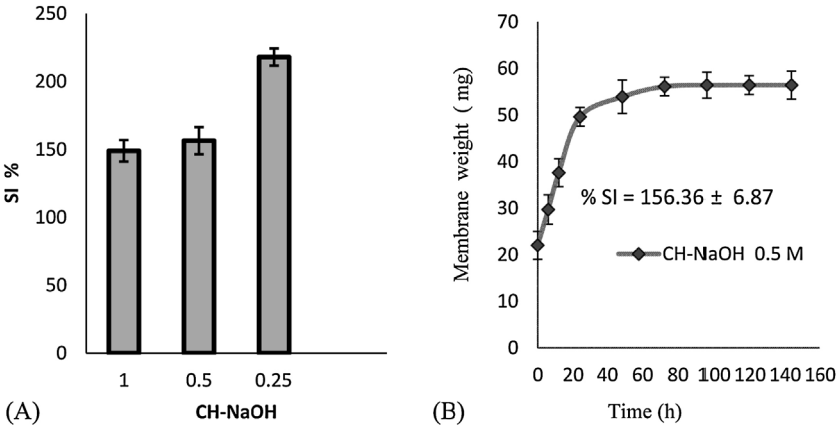

Fig. 5. (A) SI% vs. NaOH concentration and (B) water adsorption kinetics. Error bars represent SD.

agreed with the hypothesis of Okuyama et al. (1997), who revealed that water molecules were directly related to the stabilisation of CH aggregates. These water molecules were involved in the interactions between polysaccharide chains. The increase in the number of uncharged amino groups strengthens the intra-chain HO3•••O5 hydrogen bonds, causing a decrease in CH solubility.

Other properties affected by NaOH treatment were revealed during mechanical testing. Fig. 6 shows the results determined for all CH–NaOH films expressed as Young Modulus and % breaking elongation. As the NaOH concentration increases, the films that were obtained were more brittle. However, the difference between CH–0.5 NaOH and CH–1 NaOH was not statistically significant. These results were consequence of the increased interactions between polysaccharide chains conducing to films more compacted and less deformable, as was revealed in the XRD study. Also, these films showed similar or better properties of breaking elongation and tensile strength than those reported by previously (Cunha et al., 2012; Feng, Liu, Zhao, & Hu, 2012; Nam, Lee, Nam, & Lee1997; Yang, Su, Leu, & Yang, 2004; Tsai et al., 2013; He, Ao, Gong, & Zhang, 2011). These results indicated that the strength of NaOH treatment can be used as criteria for CH film structural evaluation.

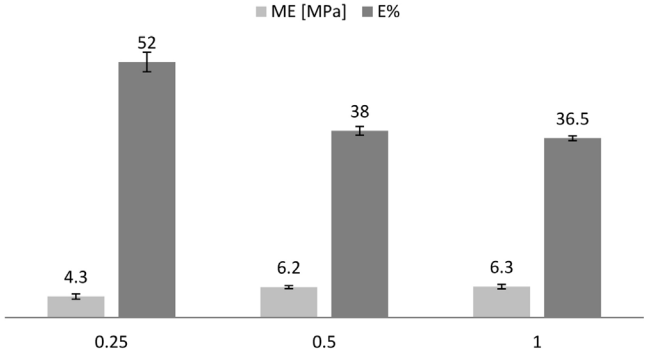

Fig. 6. Influence of the NaOH concentration on Young's modulus (ME) and on the maximum elongation (% *E*). Error bars represent SD.

4. Conclusions

CH films treated with aqueous NaOH solutions revealed that three effects were evidenced desprotonation and phosphate extraction, allowing new hydrogen bonds to form and increased CH deacetylation. X-ray diffraction patterns in CH–NaOH films revealed that two crystalline zones were present: hydrated and anhydrous polymorphs. New hydrogen bonds and fewer *N*-acetyl groups caused larger anhydrous crystal size. Moreover, a decrease in *N*-acetyl groups caused films with a more compact and disordered structure (less hydrated shells were present). Determination of the SI revealed that higher concentrations of aqueous NaOH solutions reduced the swelling in CH–NaOH films. Mechanical testing showed that the strength of NaOH treatment can be used as criteria for structural evaluation of CH films. The introduction of a mild NaOH treatment is a tool to obtain chitosan films with interesting and tunable properties.

Acknowledgements

The authors acknowledge the ANPCYT PICT 2013—No. 0367, and PROICO No. 21712 UNSL.

References

Abd-Elmohdy, F. A., Sayed, Z., Essam, S., & Hebeish, A. (2010). Controlling chitosan molecular weight via bio-chitosanolysis. *Carbohydrate Polymers*, *82*, 539–542.
Abdou, E. S., Nagy, K. S. A., & Elsabee, M. Z. (2008). Extraction and characterization of chitin and chitosan from local sources. *Bioresource Technology*, *99*, 1359–1367.
ASTM. (2010a). *Standards American Society for Testing and Materials. D882. Standard test methods for tensile properties of thin plastic sheeting*. Philadelphia, PA, USA: ASTM.
ASTM. (2010b). *Standards American Society for Testing and Materials. E96. Standard test methods for water vapor transmission of materials*. Philadelphia, PA, USA: ASTM.
Azaroff, L. A. (1968). *Elements of X-ray crystallography*. New York, NY: McGraw-Hill.
Brugnerotto, J., Lizardi, J., Goycoolea, F. M., Arguelles-Monal, W., Desbrieres, J., & Rinaudo, M. (2001). An infrared investigation in relation with chitin and chitosan characterization. *Polymer*, *42*, 3569–3580.
Cesteros Iturbe, L. C. (2004). *Revista Iberoamericana de Polímeros*, *5*, 111–132.

Chang, K. L. B., Tsai, G., Lee, J., & Fu, W. R. (1997). Heterogeneous *N*-deacetylation of chitin in alkaline solution. *Carbohydrate Research*, *303*, 327–332.

Cho, Y. W., Jang, J., Park, C. R., & Ko, S. W. (2000). Preparation and solubility in acid and water of partially deacetylated chitins. *Biomacromolecules*, *1*, 609–614.

Croisier, F., & Jérôme, C. (2013). Chitosan-based biomaterials for tissue engineering. *European Polymer Journal*, *49*, 780–792.

Cunha, R. A., Soares, T. A., Rusu, V. H., Pontes, F. J. S., Franca, E. F., & Lins, R. D. (2012). *The complex world of polysaccharides*. Croatia: Academic: InTech (Chapter 9). 10.5772/2947.

Feng, F., Liu, Y., Zhao, B., & Hu, K. (2012). Characterization of half *N*-acetylated chitosan powders and films. *Procedia Engineering*, *27*, 18–732.

Franca, E. F., Freitas, L. C. G., & Lins, R. D. (2011). Chitosan molecular structure as a function of *N*-acetylation. *Biopolymers*, *95*, 448–460.

Gopalan, N. K., & Dufresne, A. (2003). Crab shell chitin whisker reinforced natural rubber nanocomposites. 1. Processing and swelling behavior. *Biomacromolecules*, *4*, 657–665.

Harish Prashanth, K. V., Kittur, F. S., & Tharanathan, R. N. (2002). Solid state structure of chitosan prepared under different *N*-deacetylating conditions. *Carbohydrate Polymers*, *50*, 27–33.

Hasegawa, M., Isogai, A., & Onabe, F. (1993). Preparation of low molecularweight chitosan using phosphoric acid. *Carbohydrate Polymers*, *20*(4), 279–283.

He, Q., Ao, Q., Gong, Y., & Zhang, X. (2011). Preparation of chitosan films using different neutralizing solutions to improve cell compatibility. *Journal of Materials Science: Materials in Medicine*, *22*, 2791–2802.

Kaminski, W., & Modrzejewska, Z. (1997). Equilibrium studies for the sorption of metal ions onto chitosan. *Separation Science and Technology*, *32*(16), 2659.

Khor, E. (1997). Methods for the treatment of collagenous tissues for bioprostheses. *Biomaterials*, *18*, 95–103.

Knaul, J. Z., Kasaai, M. R., Bui, V. T., & Creber, K. A. M. (1998). Characterization of deacetylated chitosan and chitosan molecular weight review. *Canadian Journal of Chemistry*, *76*, 1699–1706.

Kristiansen, A., Vårum, K. M., & Grasdalen, H. (1998). The interactions between highly de-*N*-acetylated chitosans and lysozyme from chicken egg white studied by 1H-NMR spectroscopy. *European Journal of Biochemistry*, *251*, 335–342.

Kubota, N., & Eguchi, Y. (1997). Facile preparation of water-soluble *N*-acetylated chitosan and molecular weight dependence of its water-solubility. *Polymer Journal*, *29*, 123–127.

Kurita, K. (2006). Chitin and chitosan: Functional biopolymers from marine crustaceans. *Marine Biotechnology*, *8*, 203–226.

Liu, H., Adhikari, R., Guo, Q., & Adhikari, B. (2013). Preparation and characterization of glycerol plasticized (high-amylose) starch—Chitosan films. *Journal of Food Engineering*, *116*, 588–597.

Liu, W. G., Zhang, X., Sun, S. J., Sun, G. J., Yao, K. D., Liang, D. C., et al. (2003). *N*-alkylated chitosan as a potential nonviral vector for gene transfection. *Bioconjugate Chemistry*, *14*, 782–789.

Ma, B., Li, X., Qin, A., & He, C. (2013). A comparative study on the chitosan membranes prepared from glycine hydrochloride and acetic acid. *Carbohydrate Polymers*, *91*, 477–482.

Min, B., Lee, S. W., Lim, J. N., You, Y., Lee, T. S., Kang, P. H., et al. (2004). Chitin and chitosan nanofibers: Electrospinning of chitin and deacetylation of chitin-nanofibers. *Polymer*, *45*(21), 7137–7142.

Morin, A., & Dufresne, A. (2002). Nanocomposites of chitin whiskers from Riftia tubes and poly(caprolactone). *Macromolecules*, *35*, 2190–2199.

Muzzarelli, R. A. A. (1973). *Natural chelating polymers*. New York, NY: Pergamon Press.

Nam, S. Y., Lee, Y. M., Nam, S. Y., & Lee, Y. M. (1997). Pervaporation and properties of chitosan poly(acrylic acid) complex membrane. *Journal Membrane Science*, *135*, 161–171.

Nimesh, S., Saxena, A., Kumar, A., & Chandra, R. (2012). Improved transfection efficiency of chitosan–DNA complexes employing reverse transfection. *Journal of Applied Polymer Science*, *124*, 1771–1777.

Ogawa, K., Yui, T., & Miya, M. (1992). Dependence on the preparation precedure of the polymorphism and crystallinity of chitosan membranes. *Bioscience, Biotechnology, and Biochemistry*, *56*(6), 858–862.

Ogawa, K., Yuib, T., & Okuyamac, K. (2004). Three D structures of chitosan. *International Journal of Biological Macromolecules*, *34*(1–2), 1–8.

Okuyama, K., Noguchi, K., Miyazawa, T., Yui, T., & Ogawa, K. (1997). Molecular and crystal structure of hydrated chitosan. *Macromolecules*, *30*(19), 5849–5855.

Okuyama, K., Noguchi, K., Hanafusa, Y., Osawa, K., & Ogawa, K. (1999). Structural study of anhydrous tendon chitosan obtained via chitosan/acetic acid complex. *International Journal of Biological Macromolecules*, *26*, 285–293.

Osorio-Madrazo, A., David, L., Trombotto, S., Lucas, J., Peniche-Covas, C., & Domard, A. (2010). Solid-state acid hydrolysis of chitosan: Evolution of the crystallinity and macromolecular structure. *Biomacromolecules*, *11*, 1376–1386.

Paillet, M., & Dufresne, A. (2001). Chitin whisker reinforced thermoplastic nanocomposites. *Macromolecules*, *34*, 6527–6530.

Panos, I., Acosta, N., & Heras, A. (2008). New drug delivery systems based on chitosan. *Current Drug Discovery Technologies*, *5*, 333–341.

Pawlak, A., & Mucha, M. (2003). Thermogravimetric and FTIR studies of chitosan blends. *Thermochimica Acta*, *396*, 153–166.

Pearson, F. G., Marchessault, R. H., & Liang, C. Y. (1960). Infrared spectra of crystalline polysaccharides chitin. *Journal of Polymer Science*, *43*, 101.

Phongying, S., Aiba, S. I., & Chirachanchai, S. (2007). Direct chitosan nanoscaffold formation via chitin whiskers. *Polymer*, *48*, 393–400.

Ruel-Gariépy, E., Chenite, A., Chaput, C., Guirguis, S., & Leroux, J. (2000). Characterization of thermosensitive chitosan gels for the sustained delivery of drugs. *International Journal of Pharmaceutics*, *203*(1–2), 89–98.

Saito, H., Tabeta, R., & Ogawa, K. (1987). High-resolution solid state ^{13}C NMR study of chitosan and its salts with acids. *Macromolecules*, *20*(10), 2424–2430.

Schatz, C., Pichot, C., Delair, T., Viton, C., & Domard, A. (2003). Static light scattering studies on chitosan solutions: From macromolecular chains to colloidal dispersions. *Langmuir*, *19*, 9896–9903.

Schmuhl, R., Krieg, H. M., & Keizer, K. (2001). Adsorption of Cu(II) and Cr(VI) ions by chitosan: Kinetic and equilibrium studies. *Water SA*, *27*, 1–7.

Segal, L., Creely, J. J., Martin, A. E., & Conrad, C. M. (1959). An empirical method for estimating the degree of crystallinity of native cellulose using the X-ray diffractometer. *Textile Research Journal*, *29*, 786–794.

Sevel, S., Ikinci, G., & Kas, S. (2000). Chitosan films and hydrogels of chlorhexidine gluconate for oral mucosal delivery. *International Journal of Pharmaceutics*, *193*, 197–203.

Shi, Z. L., Neoh, K. G., Kang, E. T., & Wang, W. (2006). Antibacterial and mechanical properties of bone cement impregnated with chitosan nanoparticles. *Biomaterials*, *27*, 2440–2449.

Struszczyk, H. (1987). Microcrystalline chitosan. I. Preparation and properties of microcrystalline chitosan. *Journal of Applied Polymer Science*, *33*(1), 177–189.

Struszczyk, M. H. (2006). Global requirements for medical applications of chitin and its derivatives. *Polish Chitin Society; Łódź Monograph XI*, 95–102.

Tolaimatea, A., Desbrieresb, J., Rhazia, M., Alaguic, A., Vincendond, A. M., & Votterod, P. (2000). On the influence of deacetylation process on the physicochemical characteristics of chitosan from squid chitin. *Polymer*, *41*, 2463–2469.

Tsai, R. Y., Chen, P. W., Kuo, T. Y., Lin, C. M., Wang, D. M., Hsien, T. Y., et al. (2013). Chitosan/pectin/gum Arabic polyelectrolyte complex: Process-dependent appearance, microstructure analysis and its application. *Carbohydrate Polymers*, *101*, 752–759.

Wang, K., & Liu, Q. (2014). Chemical structure analyses of phosphorylated chitosan. *Carbohydrate Research*, *386*, 48–56.

Wang, Q. Z., Chen, X. G., Liu, N., Wang, S. X., Liu, C. S., Meng, X. H., et al. (2006). Protonation constants of chitosan with different molecular weight and degree of deacetylation. *Carbohydrate Polymers*, *65*, 194–201.

Wang, W., Du, Y., Qiu, Y., Wang, X., Hu, Y., Yang, J., et al. (2008). A new green technology for direct production of low molecular weight chitosan. *Carbohydrate Polymers*, *74*, 127–132.

Yang, J. M., Su, W. Y., Leu, L., & Yang, M. C. (2004). Evaluation of chitosan/PVA blended hydrogel membranes. *Journal Membrane Science*, *236*, 39–51.

Yui, T., Imada, K., Okuyama, K., Obata, Y., Suzuki, K., & Ogawa, K. (1994). Molecular and crystal-structure of the anhydrous form of chitosan. *Macromolecules*, *27*, 7601–7605.

Yui, T., Ogasawara, T., & Ogawa, K. (1995). Miniature crystal models of the anhydrous form of chitosan. *Macromolecules*, *28*, 7957–7958.

Zhang, C., Ding, Y., Ping, Q., & Yu, L. L. (2006). Novel chitosan-derived nanomaterials and their micelleforming properties. *Journal of Agricultural and Food Chemistry*, *54*, 8409–8416.